Karlsruher Institut für Technologie

Finite Element Study on Crack Terminating Angles

Gabriele Rizzi, Günter Schell, Theo Fett

KIT SCIENTIFIC WORKING PAPERS 55

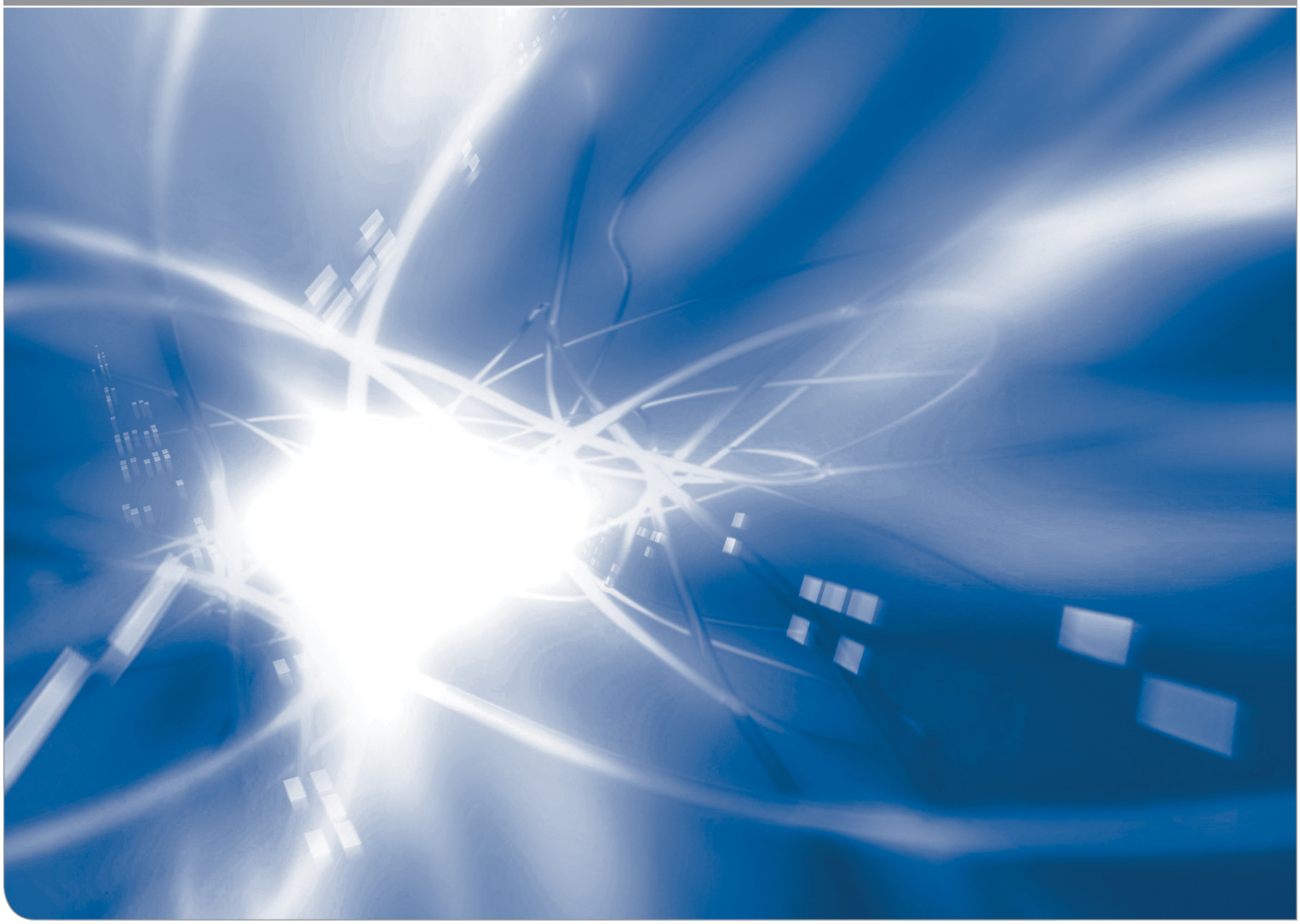

KIT – Universität des Landes Baden-Württemberg und nationales Forschungszentrum in der Helmholtz-Gemeinschaft

Institut für Angewandte Materialien, Karlsruher Institut für Technologie (KIT)

Impressum

Karlsruher Institut für Technologie (KIT)
www.kit.edu

2016

ISSN: 2194-1629

Abstract

A 3-dimensional Finite Element study has been performed on cracks which terminate at free surfaces under an angle that deviates from the straight-through crack. Such terminating angles occur when residual stresses are present in the surface region of materials. Compressive stresses let retard the crack whereas tensile stresses give rise for crack advance.

Terminating angles of 45°, 60° and 90° were studied for Poisson ratios of ν=0, 0.17, 0.20, and 0.25. The results are represented in diagrams and for an extended angle variation $0 \leq \varphi \leq 90°$ in form of polynomial approximations.

Contents

1 Introduction

Stress intensity factor solutions for fracture mechanics test specimens are mostly given under idealized simplifications which are not realized in practical applications. Handbook solutions are available predominantly for 2-dimensional crack problems with the stress state given by either “plane stress” or “plane strain”. This is equivalent to a constant stress intensity factor along the crack front.

This approximation represents the average of the stress intensity factor over the specimen thickness correctly. However, the local K-distribution will differ strongly from the average as may be demonstrated in Fig. 1a by literature results obtained in 3-dimensional FE studies. This fact is illustrated in Fig. 1a, where the local energy release rates G_{3D}, $G \propto K^2$, are plotted normalised on the G-values obtained by 2D-modelling assuming plane stress or plane strain conditions.

The squares show results of Dimitrov et al. [1] obtained for a straight crack in a 3-point bending bar. The circles are results for a “double cleavage drilled compression” (DCDC) test specimen by Fett et al. [2]. In both cases the energy release rates show a maximum in the specimen centre and significantly reduced values in the surface region.

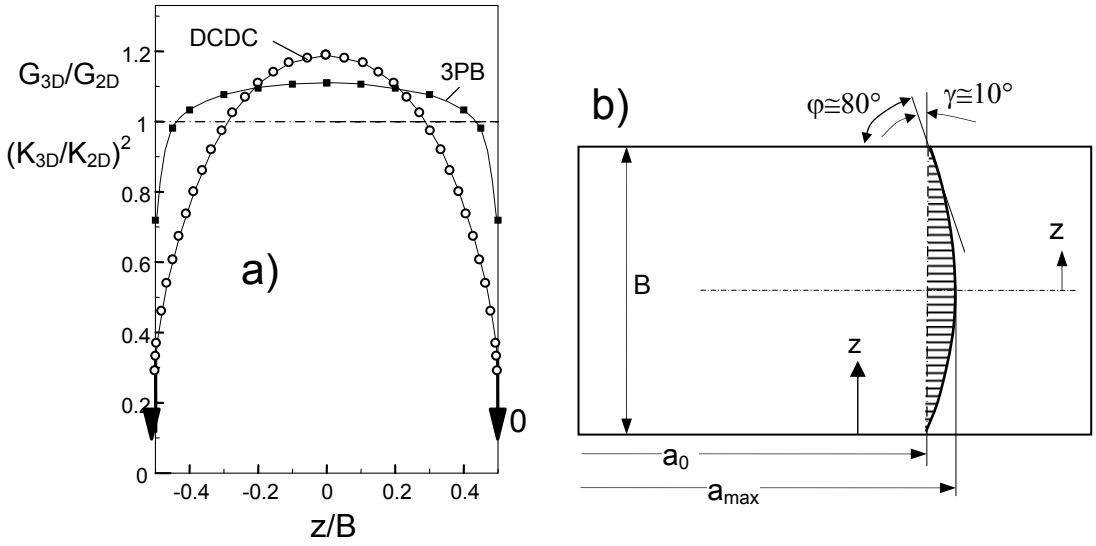

Fig. 1 a) Energy release rate distribution along the front of straight-through specimen cracks (squares: 3-point bending test [1], circles: DCDC test specimen [2]), both results obtained from FE modelling, b) crack development for the case that an angle of $\gamma \cong 10°$ is reached at the side surface (from [3]).

The problem of a crack-front intersecting a free surface is well established in theoretical fracture mechanics. Directly at the free side surface, $z \rightarrow 0$, the description of the singular stress field by a stress intensity factor is no longer possible. In this case, the stresses in a distance r from the crack tip are given by the relation

$$\sigma_y \propto r^{\lambda-1} \tag{1}$$

with in general $\lambda \neq ½$. The change of the *stress singularity* near the surface was studied very early by Benthem [4] and Bazant and Estenssoro [5].

For a crack with $\gamma = 0$ (straight crack), we obtain $\lambda \cong 0.54$ ($\nu = 0.25$) [3, 4]. The singularity exponent λ depends on the crack terminating angle γ and to a very slight extend on Poisson's ratio ν. Since $1-\lambda < 0.5$, eq.(1) yields a "weak singularity" for the stresses with $\sigma \propto r^{-0.46}$ and the consequence of a disappearing energy release rate (for details see e.g. [1]). In Fig. 1a, this result is symbolised by the arrows. It has to be emphazised that the finite *G*-values at the surface are a consequence of the finite FE-mesh. It is noteworth that the *G* reduction at the surface is stronger for the finer mesh (DCDC). A finite energy release rate, necessary for stable crack growth, is ensured only if $\gamma \cong 10°$ where $\lambda = ½$ is fulfilled for $\mu = 0.25$ and, consequently, a stress intensity factor exists. With other words: A crack can only grow <u>stably</u> at a free surface if $\gamma \approx 10°$ for $\mu = 0.25$.
From curves reported in [6] it can be concluded that the ½-singularity of stresses characterizing the stress intensity factor is only possible for a crack terminating angle of [3]

$$\varphi \cong 90° - 38.8°\nu \tag{2}$$

For most brittle materials with $\nu \approx 0.25$, the crack terminating angle is about $\varphi \approx 80°$, i.e. a deviation of 10° from the normal.

It should be emphasized that the occurrence of the singularity problem is restricted to $z = 0$ exclusively whereas for any $z \geq 0$ a *K*-value can be computed. Unfortunately, FE-structures need a finite element size so that the element closest to the surface must include the point $z=0$.

Similar to FE-computations by Newman and Raju [7] for semi-elliptical cracks, which also show a stress singularity deviating from the $1/\sqrt{r}$-type, we excluded the last element from the evaluation and extrapolated the *K*-dependency linearly to the free surface.

2 Crack terminating angle and residual stresses

The crack terminating angle at a free surface is of interest for the estimation of residual surface stresses. This behaviour was studied by 3-dimensional FE computations [3]. Figure 2a shows a crack growing from left to right in a bar with residual stresses in thin surface layers. The crack front terminates at the free surface under an angle φ, Fig. 2b. If compressive stresses (expansive strains) occur at the surfaces, the actual crack front in a crack growth test under superimposed external load must stay behind (Fig. 2c). In contrast, tensile stresses caused by shrinking effects must result in an advance of the crack (Fig. 2d).

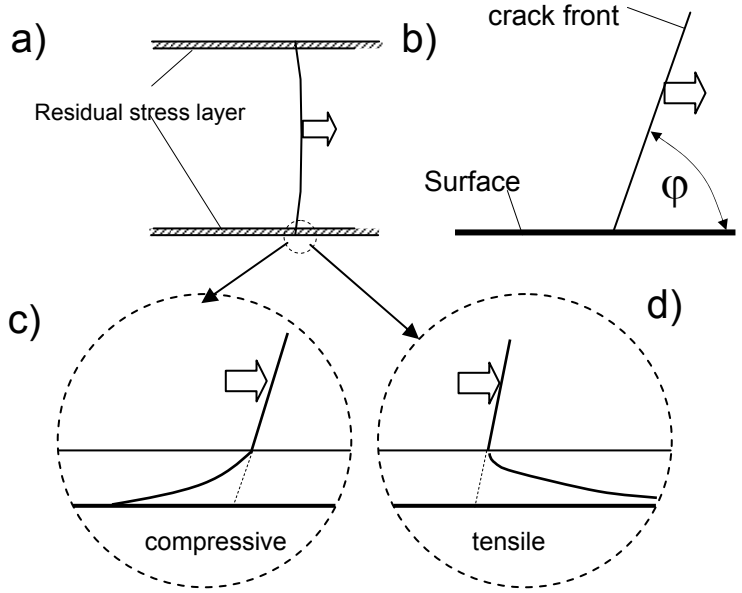

Fig. 2 a) Crack front terminating at the specimen surface under an angle φ, b) crack terminating angle, c) crack retard in a zone of compressive stresses, d) crack advance by tensile stresses. Arrows indicate crack growth direction.

3 Finite element results

3.1 Results of a previous study

In a prior study FE-computations on crack-terminating angles were performed for a material with Poisson ratio ν=0.25 as is appropriate for most ceramic materials. In this study we used a multi-sectional straight crack contour as is represented in Fig. 3a. For the computation a DCDC specimen was used with a length W=1, hole radius R=0.1 W, half width B=0.1 W, crack length a= 4R, loaded by a pressure p=1 at the ends.

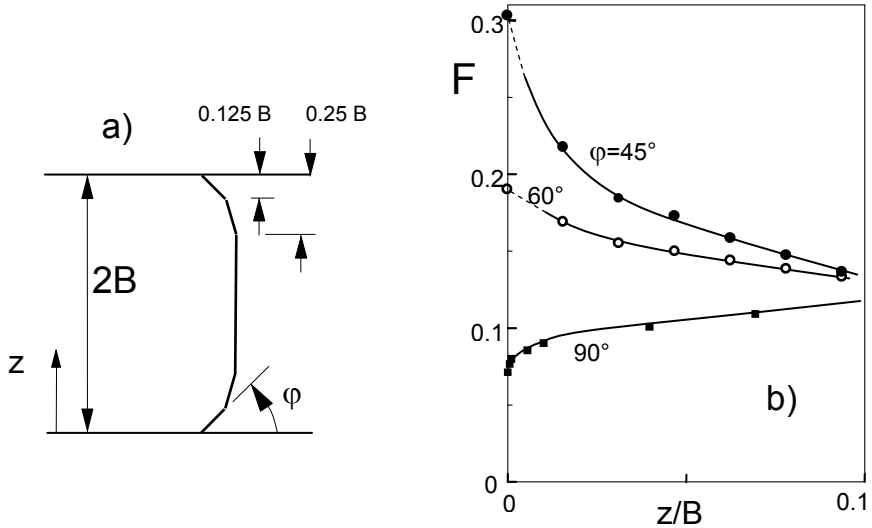

Fig. 3 a) Curved crack front approximated by straight segments, b) geometric function for the stress intensity factors near the free side surface, from [3].

The near-surface results of the geometric function F, defined by

$$K = | p | F\sqrt{\pi R} \tag{3}$$

are plotted in Fig.3b as reported in [3].

For the following FE-study, the element-mesh used in [3] was refined in the surface region by reducing the element size by a factor of 3.

3.2 Effect of Poisson's ratio

For a description of glasses the value of ν=0.25 is slightly too high. This is especially the case for silica exhibiting ν=0.17. This was the reason for extending the former FE-analysis.

First the straight crack, φ=90° may be addressed. Figure 4 shows the geometric function in the surface region for the two cases ν=0.25 and ν=0. Whereas the result from [3] shows continuously increasing stress intensity factors, the result for ν=0 is independent of the surface distance as has to be expected since disappearing Poisson ratio stands for pure plane stress conditions. In contrast to this theoretically prescribed behaviour is violated directly at the free surface, z=0. This makes clear that this deviation is an artefact of the finite element size. For studying the surface behaviour at the point z=0 the asymptotic expansion procedure is used commonly (see e.g. [6, 8]).

In Fig. 4b all different ν-values are shown considered in this study. The region of $0.2 \le \nu \le 25$ represents most glasses, for instance soda-lime glass with ν=0.22-0.23 and ν=0.17 represents silica (fused quartz). The value ν=0 is of course without technical relevance and may be applied for interpolation purposes.

The computations in [3] were carried out with ABAQUS Version 6.5 on an 8^{th} of the DCDC specimen using 20-node elements. For the straight crack 8712 elements and 40250 nodes were used. The 60°-specimen was modelled by 3540 elements and 17300 nodes and the 45°-specimen by 5600 elements and 26450 nodes. The actual study was carried out with ABAQUS Version 6.9-1 with refined meshes using 300 elements and 1350 nodes more.

Figure 5a shows the results for a crack terminating angle of φ=60° and Fig. 5b for φ=45°. The circles represent data points in the inner of the material whereas the squares indicate the extrapolations by the FE-program. Due to the extrapolation technique in ABAQUS, the squares have to be considered as estimations.

The effect of mesh refinement is shown in Fig. 6a for φ=60° and ν=0.25. It is ovious that the extrapolated stress intensity factor at the surface increases with finer mesh. This is in agreement with the expectation from eq.(1). Fenner and Mihsein [9] discussed this problem of K-determination by FE-computations in detail.

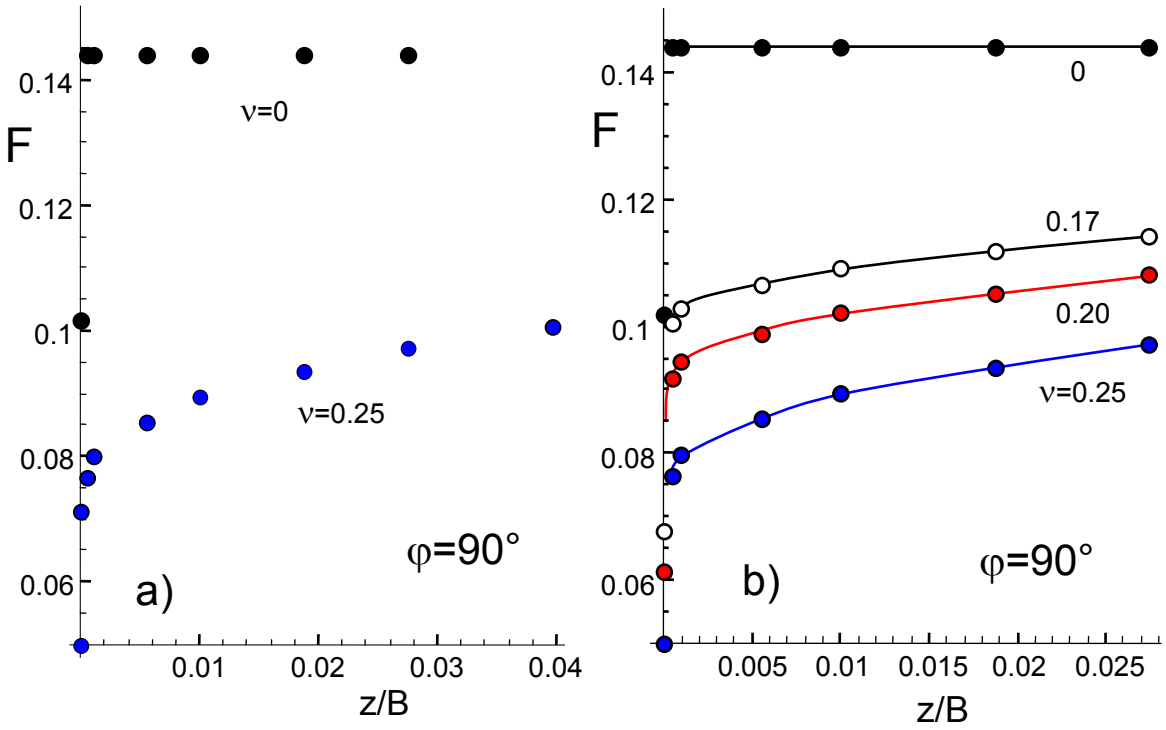

Fig. 4 Geometric function for the straight crack, a) results from [3] for ν=0.25 compared with the plane stress state realized by ν=0, b) variation of F with ν.

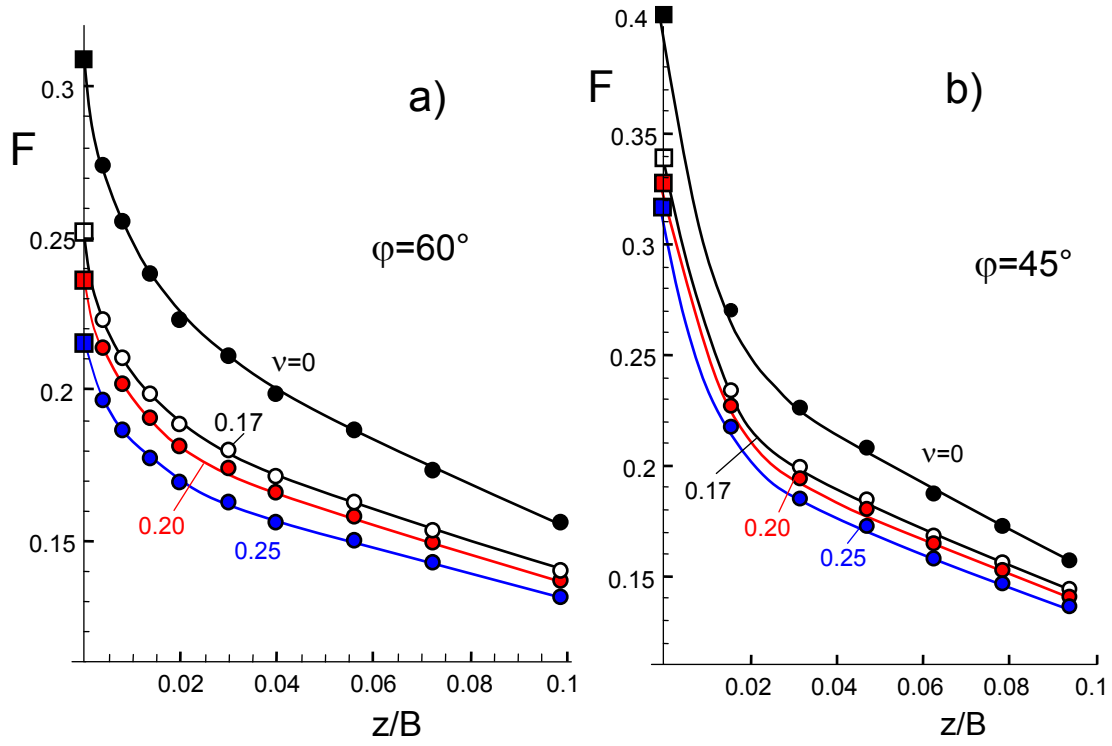

Fig. 5 Geometric function for slant cracks, a) results for φ=60°, b) for φ=45°.

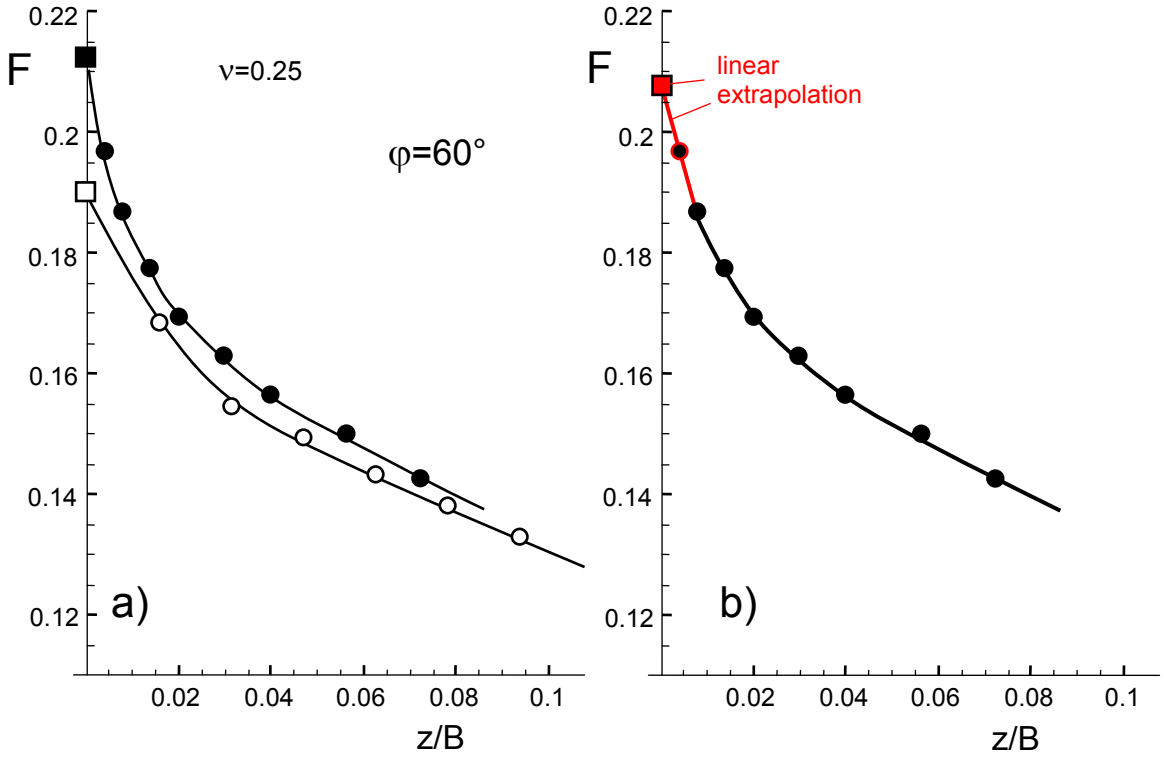

Fig. 6 a) Effect of element refinement on stress intensity factors for φ=60°, ν=0.25, b) due to the uncertainties to be expected exactly at z=0, a straight-line extrapolation of the data points closest to the surface to z=0 is recommended resulting in a lower limit for the surface stress intensity factor. The red square indicates the related stress intensity factor.

4. Stress intensity factors by linear extrapolation to z=0

Since the singularity problem appears for the limit $z\rightarrow 0$ we suggest to use stress intensity factor results only at internal elements and to extrapolate the two results closest to the surface linearly to z=0. This results in a lower limit for the surface stress intensity factor as indicated in Fig. 6b by the red square.

Figure 7a shows the linear extrapolation to the surface for all Poisson ratios ν. The extrapolations for the straight crack are illustrated in Fig. 7b.

The results for $K(\varphi)$ are plotted in a normalized form $K(\varphi)/K(90°)$ in Fig. 8a. This representation makes the results independent of the specially chosen test specimen, crack length, etc. It is therefore recommended for interpolations in the ranges $45° \le \varphi \le 180°$ and $0 \le \nu \le 0.25$.

For extrapolations in the region $\varphi \le 45°$ the reciprocal stress intensity factor ratio as the ordinate of Fig. 8b may be recommended, $K(90°)/K(\varphi)=0$. In this case it can be used in addition: $K(0°)/K(90°)\rightarrow\infty$, i.e. $K(0°)/K(90°)=0$ (see e.g. [9]). Figure 8b shows the results together with interpolation curves which are given by eqs.(4-7).

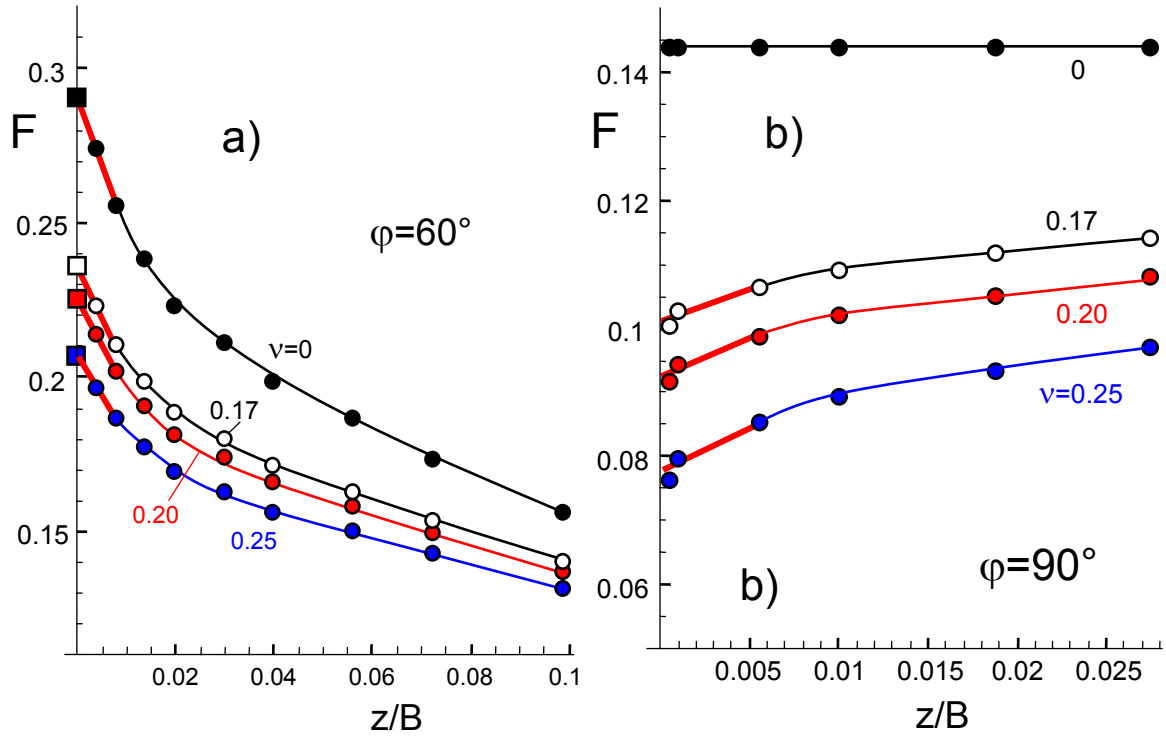

Fig. 7 Linearly extrapolation of stress intensity factors from internal elements to the surface indicated by the thick red line parts, a) for φ=60°, b) for φ=90°.

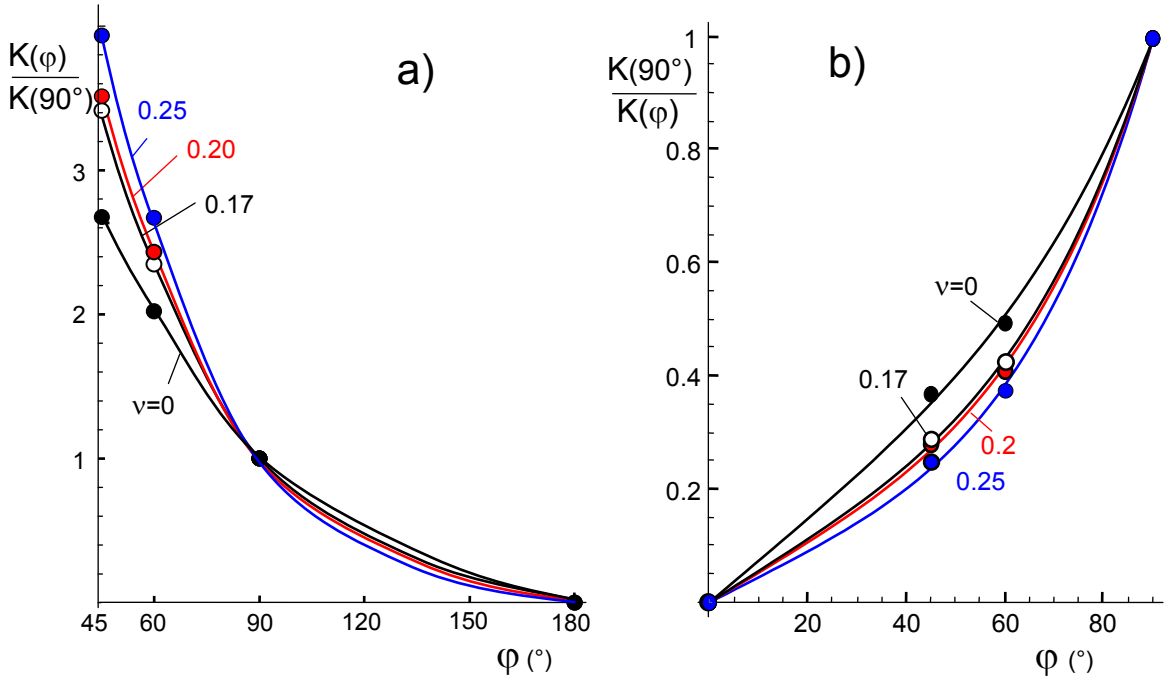

Fig. 8 a) Stress intensity factors normalized on values for the straight crack, b) reciprocal representation for an evaluation of cracks including the region φ<45°.

The data of Fig. 8b may be approximated as:

ν=0.25
$$\frac{K(\varphi)}{K(90°)} \cong \frac{1}{0.00451\,\varphi + 9.03\times10^{-9}\,\varphi^4} \tag{4}$$

ν=0.20
$$\frac{K(\varphi)}{K(90°)} \cong \frac{1}{0.00533\,\varphi + 7.98\times10^{-9}\,\varphi^4} \tag{5}$$

ν=0.17
$$\frac{K(\varphi)}{K(90°)} \cong \frac{1}{0.00562\,\varphi + 7.52\times10^{-9}\,\varphi^4} \tag{6}$$

ν=0
$$\frac{K(\varphi)}{K(90°)} \cong \frac{1}{0.00745\,\varphi + 4.98\times10^{-9}\,\varphi^4} \tag{7}$$

Figure 9 represents an interpolation for $\nu = 0.225$ (soda-lime glass) where the circles are the interpolated FE-results. The dependency including the limit case for $\varphi = 0$ can be expresessed by the polynomial equation

ν=0.225
$$\frac{K(\varphi)}{K(90°)} \cong \frac{1}{0.00497\,\varphi + 8.39\times10^{-9}\,\varphi^4} \tag{8}$$

for the angle φ in degree. Equation (8) is plotted in Fig. 9 as the curve.

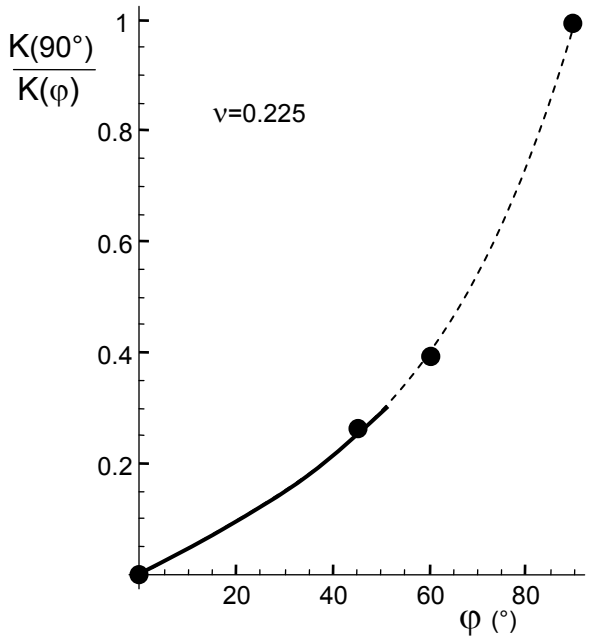

Fig. 9 Reciprocal representation of stress intensity factors for an interpolated Poisson ratio of ν=0.225 as is usual for instance for soda-lime glass. This diagram is recommended for evaluations in the region φ<45°.

In a rather rough approximation the general dependency can be expressed for $\varphi \le 90°$ and $0 \le \nu \le 0.25$ by:

$$\frac{K(\varphi)}{K(90°)} = \frac{1}{c_0(\nu)\varphi + c_1(\nu)\varphi^4} \tag{9}$$

with the coeffecients

$$c_0 \approx 0.00749 - 0.01139\ \nu \tag{10}$$

$$c_1 \approx (4.928 + 15.8\ \nu) \times 10^{-9} \tag{11}$$

References

1 Dimitrov, A., Buchholz, F.-G., Schnack, E., "3D-corner effects in crack propagation." In H.A. Mang, F.G. Rammerstorfer, and J. Eberhardsteiner, eds, *On-line Proc. 5th World Congress in Comp. Mech. (WCCMV)*, Vienna, Austria, July 7–12(2002); http://wccm.tuwien.ac.at.

2 Fett, T., Rizzi, G., Guin, J.P., López-Cepero, J.M., Wiederhorn, S.M., A fracture mechanics analysis of the DCDC test specimen, Engng. Fract. Mech. **76**(2009), 921-934.

3 Fett T. Stress intensity factors, T-stresses, Weight function (Supplement Volume), IKM **55**, KIT Scientific Publishing, Karlsruhe; 2009; (Open Access: http://digbib.ubka.uni-karlsruhe.de /volltexte/1000013835).

4 Benthem, J.P., "State of stress at the vertex of a quarter-infinite crack in a half-space," *Int. J. Solids and Struct.* **13**(1977),479.

5 Bazant, Z.P., Estenssoro, L.F., "Surface singularity and crack propagation," *Int. J. Solids and Struct.*, **15**(1979)**,** 405-426.

6 Dimitrov, A., Eckensingularitäten bei räumlichen Problemen der Elastizitätstheorie: Numerische Berechnung und Anwendungen, PhD-Thesis, University of Karlsruhe, 2002.

7 Newman, J.C., Raju, I.S., An empirical stress intensity factor equation for the surface crack, Engng. Fract. Mech. **15**(1981), 185-192

8 Dimitrov, A., Buchholz, F.-G., Schnack, E., "On three-dimensional effects in propagation of surface-breaking cracks, CMES, Comp. Mod. in Engng.& Science **12**(2006),1-25.

9 Fenner, D.M., Abdul Mihsein, M.J., Crack front elastic stress state for three-dimensional crack problems, International Journal of Fracture **25** (1984) 121-131.

KIT Scientific Working Papers
ISSN 2194-1629

www.kit.edu